

Influence of V(C,N) precipitates on microstructure and mechanical properties of continuous cooled C-Mn-V

CARLOS Garcia-Mateo, CARLOS Capdevila, JUAN Cornide, JESUS Chao, FRANCISCA G. Caballero and CARLOS Garcia de Andres

(MATERIALIA Research Group. Department of Physical Metallurgy, Centro Nacional de Investigaciones Metalúrgicas (CENIM-CSIC), Avda. Gregorio del Amo, 8. E-28040 Madrid, Spain)

Abstract: The effect of chemical composition and processing parameters on the formation of acicular ferrite and/or bainite has been investigated. In particular, this paper deals with the influence that N through its combination with V, as V(C,N) precipitates, has on the decomposition of austenite. Likewise, the intragranular nucleation potency of V(C,N) precipitates is analyzed through the continuous cooling transformation diagrams (CCT) of two C-Mn-V steels with different contents of N.

Results reported in this work allow us to conclude that acicular ferrite can only be achieved alloying with vanadium and nitrogen, meanwhile bainite is promoted in steels with a low level of nitrogen. It is concluded that higher strength values are obtained in acicular ferrite than in bainitic steel but a similar brittle-ductile transition temperature (BDT), and lower values of impact absorbed energy (KV) has been recorded in nitrogen-rich steel.

Key words : acicular ferrite, bainite, vanadium precipitates, mechanical properties.

Nowadays it is well known the beneficial aspects of acicular ferrite (AF) as compare with bainite (B) in terms of mechanical properties. Both form in the same temperature range and by the same type of transformation mechanism^[1-3]. In the case of bainite, the ferrite nucleates at the austenite grain boundaries and forms packets of parallel plates with similar crystallographic orientations, whereas acicular ferrite nucleates intragranularly. Therefore, acicular ferrite plates exhibit different spatial orientations and, as a consequence, a more chaotic arrangement, showing fine-grained interlocking morphologies, which affects favorably both, strength and toughness.

Typical nucleation sites for acicular ferrite are a mixture of the oxidation products of manganese, silicon, titanium, plus sulphides, nitrides and carbides^[4], or incoherent MnS +V(C, N) complex precipitates^[5-8]. In this work, different combination of nitrogen and vanadium contents have been analysed from the AF nucleation potency point of view. Therefore, this work deals with the detrimental or beneficial aspects of alloying the steel with vanadium and nitrogen in order to promote the formation of acicular ferrite or bainite, and their mechanical response.

1 Experiment Method

The combined effect of V and N on AF formation has been analyzed by studying the austenite decomposition in two laboratory grades, see Table 1. The base composition is the same for both alloys differing only in the N content.

A high resolution dilatometer Adamel Lhomargy DT1000 has been used to determine the CCT diagrams of these steels.

An austenitisation temperature of 1125 °C was used for both steels, this way the measured prior austenite grain size (PAGS) in both steels is the same $\approx 60 \mu\text{m}$, ruling out from the study its influence on the formation of AF or B and their final properties.

Microstructural observation has been performed, after standard sample preparation, with a JEOL JSM6500 field emission gun scanning electron microscope (FEG-SEM).

Tensile specimens with a section 3 mm in diameter and a gage length of 16 mm were tested at room temperature using a Microtest EM2/100/FR testing machine fitted with a 100-kN load cell. A crosshead speed of $8.3 \cdot 10^{-3} \text{ mm s}^{-1}$ was used in all the experiments. From the engineering stress-strain curves, 0.2 pct yield stress (YS), ultimate tensile strength (UTS), uniform elongation, (ϵ_u) and total elongation (ϵ_T) were obtained.

Subsized V-notch (2 mm in depth) Charpy specimens $10 \times 2.5 \times 55 \text{ mm}^3$ in size were machined and tested according to the standards^[9] using a pendulum of 147 J of capacity and with a hammer velocity of 5.4 m s^{-1} in the instant of impact. In order to provide the ductile-brittle transition (DBT) temperature Charpy tests were carried out between RT & -196°C. The results presented correspond to an average of three tests.

Table 1. Chemical compositions of the experimental grades, all in wt%.

Grade	C	Mn	V	N	Al	Si	Ti	S
4B	0.080	1.46	0.25	0.0016	0.020	0.004	0.001	0.001
5B	0.080	1.46	0.25	0.0180	0.016	0.007	0.001	0.001

2 Results and Discussion

2.1 Microstructural analysis

The CCT diagrams thus obtained for 4B and 5B steels are presented in Fig. 1. Where it is possible to observe that in the case of 4B steel AF is not the major decomposition product at any of the cooling rates tested. This behavior could be related with the low nitrogen content and the absence of S which avoids the formation of MnS inclusions, as it will be shown below. On the other hand, the addition of N (5B steel) results in an optimal combination of V and N to induce the massive formation of acicular ferrite, and even overcome the absence of MnS inclusions. However the continuous cooled microstructure is a mixture of proeutectoid ferrite, pearlite, B, AF and martensite in different proportions depending on the cooling rate. With the aim of obtaining an homogeneous microstructure, either of AF or B, a two-step cooling heat treatment was designed in accordance with the CCT diagrams, i.e accelerated cooling is finished at 630 °C, and then the sample is cooled down to room temperature at 2°C/s in order to maintain the steel inside the AF or B field (5B and 4B respectively) as long as possible, but with a relative small risk of some proeutectoid ferrite formation. By doing so the achieved microstructures are mainly of AF in 5B steel and of B in 4B steel as Fig. 2 demonstrates. It is clear from above mentioned results the relationship between V(C,N) precipitates and acicular ferrite formation.

The V(C,N) particles can precipitate on pre-existent MnS inclusions or within austenite. In this sense, Fig. 3 shows MTDATA calculations where it is clear that the presence of MnS is almost negligible in both steels. Therefore V(C,N) precipitation should take place within austenite. In the case of 5B precipitation starts at much higher temperatures than in 4B steel, see Fig.3, meaning that effectively the amount of precipitation in 5B as compare with 4B is also higher, which may explain the increase in AF fraction. It is also noticeable that with an increasing N content, a higher amount of V is tied up, thus, a lower amount of V will combine with carbon to form V carbides. Hence, the excess of carbon in 5B steel as compared to 4B steel will trigger the interlath cementite precipitation, as shown in Fig. 2 and Fig. 4. Cementite laths are precipitated in the boundary between the ferrite plate and austenite during the growth of acicular ferrite plates. As transformation proceeds, carbon is depleted from the ferrite plate to austenite and the carbon coming from adjacent ferrite plate is accumulated into the untransformed austenite; once it is saturated in carbon cementite precipitation occurs.

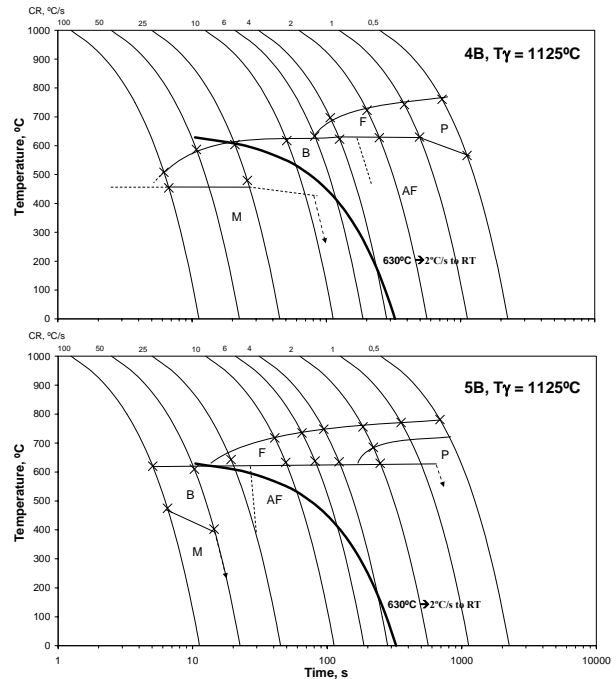


Fig 1. CCT diagrams. Also represented the 2°C/s cooling rate applied after accelerating cooling (50 °C/s) from T_γ to 630 °C.

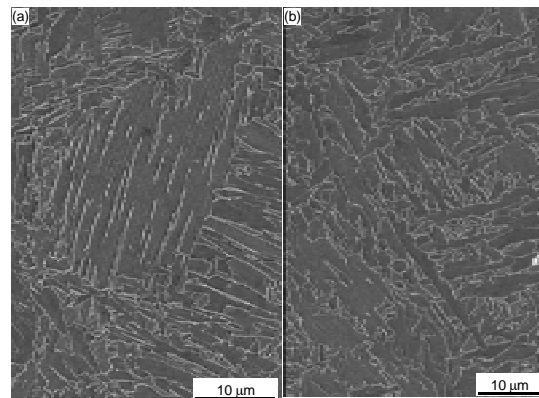


Fig.2 FEG-SEM micrographs of the developed microstructures after the two step cooling treatment in (a) 4B, fully bainitic, and (b) 5B AF microstructure. Images also show cementite precipitation as light gray platelets on ferrite interlath.

Moreover, the carbon that does not diffuse away from the ferrite is trapped inside and promotes a second precipitation process in the form of very fine precipitates (likely to be vanadium carbides) inside the ferrite plates, as is seen in Fig. 4.

As it will be shown later in this work, the presence of cementite is expected to deteriorate the toughness behavior of 5B, as cementite is regarded as a hard and brittle phase.

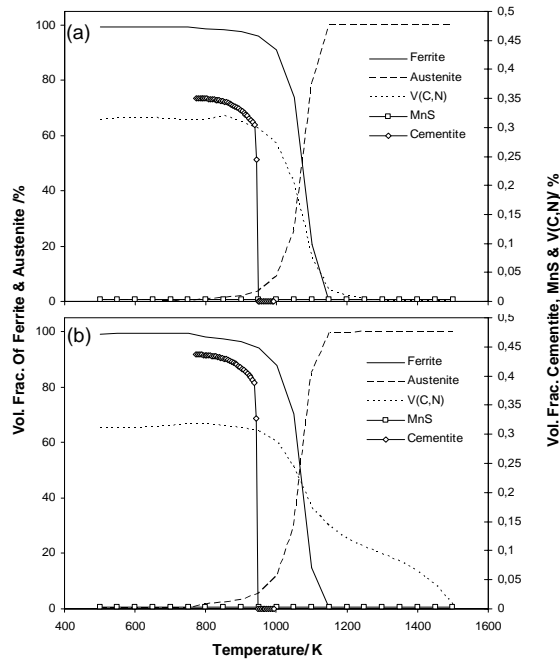


Fig.3. Evolution of phases in (a) 4B and (b) 5B steels.

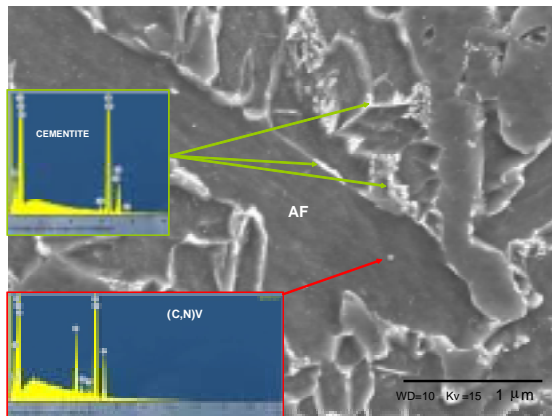


Fig.4. FEG-SEM image of 5B steel showing nucleation of acicular ferrite in V(C,N). Also shown cementite features.

2.2 Tensile tests results & impact absorbed energy tests

Results corresponding to tensile tests are presented in Table 2, and correspond to an average of two tests. 5B steel, with AF microstructure, exhibits higher strength levels than that measured for the bainitic microstructure attained in 4B steel.

Regarding to ϵ_u and RA values, it is worth noting the behaviour of 5B steel, which achieving higher strength values maintain the same ductility values than the bainitic steel. Finally, it could be concluded that the higher misorientation between ferrite plates and the higher amount of precipitates (cementite and V(C,N)) leads to higher values of YS and UTS maintaining the same levels of elongation in 5B steel as compare to 4B.

Table 2. Summary of mechanical properties. RA stands for the reduction in area, ϵ_u stands for uniform elongation and ϵ_t for total elongation, all in %. YS and UTS are in MPa.

	YS	UTS	ϵ_u	ϵ_t	RA
5B	515	633	6	26	75
4B	462	572	5.5	25	74

Impact absorbed energy tests were carried out in 4B and 5B steels at temperatures ranging from room temperature to -196°C , results thus obtained are presented in Fig. 5.

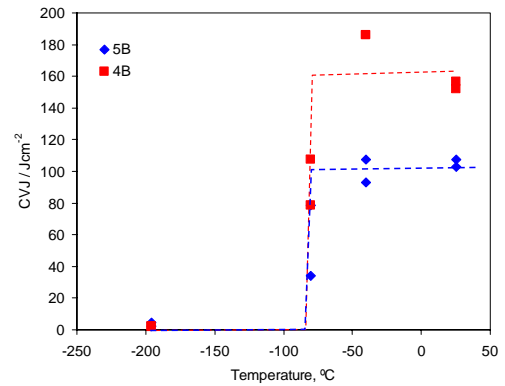


Fig.5. Ductile-Brittle transition temperature in 4B and 5B steels after two-step cooling.

As AF plates radiates in many directions from the point nucleation site with highly misoriented plates and bainite presents a more parallel arrangements of plates, the expected *effective grain size* should be smaller in the case of 5B than in 4B.

Giving that there is not free N that may impair toughness^[10,11], as MTDATA predicted is all tight with V, toughness results could be rationalised as follows.

The upper-shelf results reveals that 4B steel presents the highest value of energy in the upper shelf. As is well known, in this region of the DBT curve, the fracture occurs through the nucleation, growth, and coalescence of microvoids. The fracture event takes place at the point at which a critical plastic strain is reached on a microstructure-related critical distance^[12]. The critical strain is a function of the microstructure (the morphology, size, and distribution of the inclusions) and the stress triaxiality state^[13,14]. Moreover, for similar microstructural states, the energy in the upper-shelf region decreases with an increase in the strength level of the steel^[15]. Therefore, the lower absorbed-energy value recorded for 5B steel can be attributed, partially, to the higher YS of this steel (Table 2), because both 4B and 5B steels have a similar inclusionary state (Fig. 3). In addition, the presence of a higher fraction of cementite, hard and brittle phase, in 5B steel adds up to the observed toughness deterioration. On the other hand, the Charpy energy values at -196°C of both steels are very similar, as it is the DBT temperature of both steels, around -80°C .

3 Conclusions

- Two S-lean laboratory heats and different N additions (5B steel for a high N content and 4B for a low N content) have been studied. The FEG-SEM observations revealed that V precipitates act as nucleation sites for acicular ferrite in the absence of sulfide inclusions.

- The microstructural analysis revealed that VN precipitation seems to enhance the formation of acicular ferrite structure (5B steel), whereas VC leads to a lathlike bainitic structure (4B steel).

- The 5B steel presents higher YS and UTS values than the 4B steel, without a significant decrease in elongation. Thus, 5B steel presents the best combination of strength and ductility.

- The higher energy value of the upper shelf of 4B as compared to 5B steel can be explained on the basis of the lower YS value.

- In addition to the smaller effective grain size for 5B than for 4B steel, similar transition temperatures for both steels have been recorded. This fact is strongly related to the amount of cementite precipitated between ferrite laths, which is higher in 5B than in 4B steel.

4 Acknowledgements

The authors would like to express their gratitude to VANITEC and the Spanish Ministerio de Ciencia e Innovacion for their financial support.

References:

- [1] Babu S.S. and Bhadeshia H.K.D.H. Stress and the Acicular Ferrite Transformation. *Mater. Sci.Eng. A*, 1992 156: 1-9.
- [2] Capdevila C. Ferrer J.P, Garcia-Mateo C., Caballero F.G., López V. and García de Andrés C. Influence of Deformation and Molybdenum Content on Acicular Ferrite Formation in Medium Carbon Steels. *ISIJ Int.* 2006, 46 : 1093-1100.
- [3] Capdevila C., Caballero F.G. and García de Andrés C. Isothermal Allotriomorphic Ferrite Formation Kinetics in a Medium Carbon Vanadium-Titanium Microalloyed Steel. *Scr. Mater.* 2001, 44: 593-600..
- [4] Zhang Z, Farrar R. A. Role of non-metallic inclusions in formation of acicular ferrite in low alloy weld metals . *Mater. Sci.Technol.* 1996,12 :237-260.
- [5] Ishikawa F., Takahashi T. and Ochi T. Intragranular Ferrite Nucleation in Medium-Carbon Vanadium Steels. *Metall. Trans. A.*1994, 24A : 929-936.
- [6] Capdevila C., Caballero F.G. and García de Andrés C. Modeling of Kinetics of Isothermal Idiomorphic Ferrite Formation in a Medium-Carbon Vanadium-Titanium Microalloyed Steel. *Metall. Trans A.* 2001, 32: 1591-1597.
- [7] Capdevila C., Caballero F.G., García-Mateo C. and García de Andrés C. The Role of Inclusions And Austenite Grain Size On Intergranular Nucleation Of Ferrite In Medium Carbon

Microalloyed Steels. *Metall. Trans. A.* 2004,45: 2678-2685.

[8] Zajac S., Medina S. F., Schwinn V., Osta A., De Sanctis M., Herman G., Final Report EUR 22451 EN, Directorate General for Research, Luxembourg, 2007, ISBN 92-79-04814-2.

[9] ASTM E-399 Standard Test Method for Plane Strain Toughness of Metallic Materials. *Annual Book of ASTM Standard*, 1995, 03.01: 412-442

[10] Yamane T., Hisayuki K., Kawazu Y., Takahashi T., Kimura Y., Tsukuda S. Improvement of toughness of low carbon steels containing nitrogen by fine microstructures, *J. Mater. Sci.* 2002, 37: 3875-3879.

[11] Bang K. S., Park C., Liu S. Effects of nitrogen content and weld cooling time on the simulated heat-affected zone toughness in a Ti-containing steel. *J. Mater. Sci.* 2006,41: 5994-6000.

[12] Pineau A.: In *Advances in Fracture Research ICF5*, D. Francois, ed., Pergamon Press, Oxford, United Kingdom, 1982: 553-577.

[13] Mackenzie A.C, Hancock J.W, and Brown D.K. On the influence of state of stress on ductile failure initiation in high strength steels, *Eng. Fract. Mech.*, 1977, vol. 9, pp. 167-168.

[14] Lautridou J.C. and Pineau A.. Crack initiation and stable crack growth resistance in A508 steels in relation to inclusion distribution. *Eng. Fract. Mech.* 1981,15: 55-71.

[15] Speich G.R. and Spitzing W.A. Effect Of Volume Fraction And Shape Of Sulfide Inclusions On Through-Thickness Ductility And Impact Energy Of High-Strength 4340 Plate Steels. *Metall. Trans. A.* 1982, 13:, 2239-2258.

